THE ABSORPTION AND FLUORESCENCE OF ANTHRACENE IN THE NEAR ULTRA-VIOLET

by

SEIKO KATAGIRI

B. En., The University of Niigata, Japan, 1962

A THESIS SUBMITTED IN PARTIAL FULFILMENT OF

THE REQUIREMENTS FOR THE DEGREE OF M. Sc.

in the Department

of

Chemistry

We accept this thesis as conforming to the

required standard

THE UNIVERSITY OF BRITISH COLUMBIA

April, 1964

In presenting this thesis in partial fulfilment of the requirements for an advanced degree at the University of British Columbia, I agree that the Library shall make it freely available for reference and study. I further agree that permission for extensive copying of this thesis for scholarly purposes may be granted by the Head of my Department or by his representatives. It is understood that copying or publication of this thesis for financial gain shall not be allowed without my written permission.

Department of Chemistry

The University of British Columbia,
Vancouver 8, Canada

Date May 6, 1964

ABSTRACT

The fluorescence and absorption spectra of anthracene in the near ultra-violet were investigated in n-heptane, fluorene, biphenyl and n-hexane matrices at low temperature. The assignment of the excited electronic state as $^1B_{1u}$ was confirmed. In the ground electronic state eight a_g and five b_{3g}, and in the $^1B_{1u}$ upper electronic state seven a_g and five b_{3g} fundamentals were assigned. It was deduced that the potential surfaces of the ^1A_g and the $^1B_{1u}$ states were similar in shape as there was an approximate agreement between the values of corresponding fundamental vibrations in the two electronic states. The potential surfaces were unusually harmonic for a polyatomic molecule, at least along the normal co-ordinates available to this study. No evidence for the presence of anharmonicity was found in even the highest overtone (the third) measured, although several possible examples of Fermi resonance between vibrational modes were observed both in fluorescence and in absorption. The Fermi resonances were assigned primarily on the basis of intensity transfer between lines rather than line shifts. The presence of a weaker long-axis polarized transition ($^1B_{2u} \leftarrow {}^1A_g$) in anthracene predicted by theory was not detected.

The lowest energy electronic transition in fluorene was found to be polarized along the long axis of this molecule.

ACKNOWLEDGMENT

I am deeply grateful to Dr. Alan V. Bree for his guidance and encouragement in every phase of this work; his assistance has developed my interest and understanding in the work.

I wish to express my appreciation to Miss V.V.B. Vilkos for her help in many ways, and also to the technicians in this department for the preparation of some equipment.

CONTENTS

Page

TABLES

FIGURES

SURVEY OF PREVIOUS WORK

Theoretical Predictions

Electronic States of Anthracene

Group theory may be usefully applied to the calculation of the molecular orbitals (MO's) of an anthracene molecule using as a basis set the atomic $2p_x$ functions centred on each carbon nucleus. Anthracene possesses D_{2h} molecular symmetry and its character table and axis convention are shown below. It can be shown (1) that the one-electron MO's are A_u, B_{1g}, B_{2g} and B_{3u} yielding the configurations A_g, B_{1u}, B_{2u} and B_{3g}.

According to Weissman (2) antisymmetric spin functions have A_g symmetry, so singlet π - electron configurations retain the symmetry given above. Thus the only allowed transitions arising from the A_g ground state are to B_{1u} and B_{2u} excited states polarized along the long and short axis of the molecule, respectively.

Many calculations (3)-(13) have been carried out on the energies of the electronic transitions of anthracene and the corresponding oscillator strengths (f) in different approximations (e.g. allowing for the interaction between many configurations, the inclusion of many-centred integrals

Table 1

Character Table of D2h and the Axis Convention of the Anthracene Molecule

D2h	E	C_2^x	C_2^y	C_2^z	i	σ^{yz}	σ^{zx}	σ^{xy}	T	R
Ag	1	1	1	1	1	1	1	1		
Au	1	1	1	1	-1	-1	-1	-1		
B1g	1	-1	-1	1	1	-1	-1	1		Rz
B1u	1	-1	-1	1	-1	1	1	-1	Tz	
B2g	1	-1	1	-1	1	-1	1	-1		Ry
B2u	1	-1	1	-1	-1	1	-1	1	Ty	
B3g	1	1	-1	-1	1	1	-1	-1		Rx
B3u	1	1	-1	-1	-1	-1	1	1	Tx	

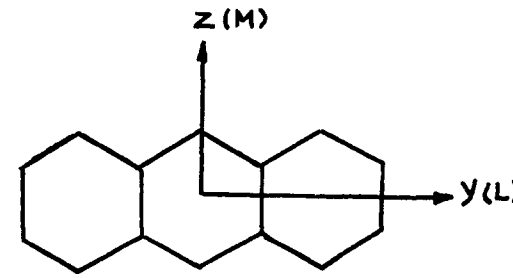

in the secular equation, etc.). All calculations put only $^1B_{1u}^+$ and $^1B_{2u}^-$ levels in the region of the 3800 Å system. Only one calculation (9) found the $^1B_{2u}^-$ level lower than $^1B_{1u}^+$. The oscillator strength of the $^1B_{1u}^+ \leftarrow {}^1A_g^-$ transition was much higher than that of the $^1B_{2u}^- \leftarrow {}^1A_g^-$ in every approximation, and for the latter Pariser (8) and Mataga (10) calculated zero.

Table 2

A Summary of Some Calculations on the Electronic States of Anthracene in the Near Ultra-Violet

	ref.	$^1B_{1u}^+$ (∥M)	f	$^1B_{2u}^-$ (∥L)	f	
V.B.	3			3.07 ev		
M.O.	4	0.836 γ		1.261 γ		γ =resonance integral
	5		0.11		0.005	
Modified	6,7	3.72 ev	0.10			
MO Methods	8	3.6	0.4			

Table 2 continued

	ref.	$^1B_{1u}^+$ (IIM)	f	$^1B_{2u}^-$ (IIL)	f	
		ev		ev		
Modified	9	3.6		3.2		
MO Methods	10	3.48	0.39	3.91	0.00	
	11	3.15				
	12	3.44	0.283	3.51	0.116	TBX Approximation
		3.44	0.265	3.61	0.063	IRX Approximation
		3.23	0.395	3.51	0.162	TBM Approximation
		3.15	0.290	3.63	0.087	IRM Approximation
	13	3.31-3.47				

Vibrational States of Anthracene

The anthracene molecule has 66 fundamental vibrational modes classified as 12 a_g, 5 a_u, 4 b_{1g}, 11 b_{1u}, 6 b_{2g}, 11 b_{2u}, 11 b_{3g} and 6 b_{3u}. Among them only a_g and b_{3g} modes are expected to be built on the allowed B_{1u} and B_{2u} origins by vibrational perturbation of the electronic transitions.

No calculations of the energies of the fundamental vibrations have been reported. However, a_g and b_{3g} fundamentals are active in Raman spectra and so any available data may be consulted to aid in the assignment of the vibrational structure in fluorescence.

The energy deviation of combination bands from their harmonic value can occur due to anharmonicity of the potential field in the molecule. For accidentally degenerate or very close lying vibrational levels the anharmonicity gives rise to a Fermi resonance (14) which causes a splitting of the two degenerate levels, or a further separation of two levels of the same symmetry. These two effects (anharmonicity and

Fermi resonance) are mentioned here because they might be expected to appear in the observed spectra.

The matrix element of the dipole moment operator M is defined as (15)

$$M = \int m \, \sigma''^{*}_{nucl} \, \sigma'_{nucl} \, d\tau_{nucl}$$

where $m = \int \psi''^{*}_{el} \hat{M} \psi'_{el} \, d\tau_{el}$. The initial and final vibrational wave functions σ''_{nucl} and σ'_{nucl} are stationary state functions of a many-dimensional oscillator. The Franck-Condon principle states that m does not depend on the coordinates of the nuclei. At a sufficiently low temperature the molecule normally exists in its vibrationless ground state, and since only those transitions are possible for which the overlap integral $\int \sigma''^{*}_{nucl} \, \sigma'_{nucl} \, d\tau_{nucl}$ does not vanish, totally symmetric vibrations are active in the upper state. For anthracene these are a_g fundamentals or any odd overtone.

Although the intensity of a line is given by M^2, it cannot be predicted because the overlap integral depends on the change in geometry of the molecule between the ground and the excited states which is not known. Conversely from the observed intensities of members of a vibrational progression, changes in molecular dimensions may be dis - cussed. (16),(17).

Mixed Crystal Phenomena

If the solute molecule does not interact with the surrounding solvent molecules that make up the host crystal lattice, then the solute molecules may be regarded as an "oriented gas". The solvent molecules would then only serve to hold the guest molecules in a fixed orientation in space and the observed spectrum would be identical with the free molecule spectrum observed in the vapour phase. However, various modifications on the free molecule spectrum are found in the mixed crystal spectrum and these arise from the perturbations caused by the surrounding solvent molecules (18) (19). These are (i) a shift of the entire spectrum to the red or to the blue and (ii) a change in the intensities of the individual lines in the spectrum due to intensity stealing from other nearby systems. Effect (i) is difficult to predict and only one calculation has been made (20); calculations of effect (ii) have been made using second-order perturbation theory for some systems (21).

Shpol'skii (22) (23) has shown that well-resolved spectra of organic molecules may be obtained in normal paraffin solid solution at 77°K. This method provides an abundance of precise data concerning the vibrational structure of electronic states. A theoretical treatment of the Shpol'skii effect has been presented by Rebane and Khizhnyakov (24) (25).

Previous Experimental Work

All previous workers have interpreted the 3800 A° absorption system of anthracene as arising solely from a $^1B_{1u}^+ \leftarrow {}^1A_g^-$ transition. The predicted $^1B_{2u}^- \leftarrow {}^1A_g$ transition has not been observed. The system has been analysed in the vapour (26), solution (27), solid solution (28) and crystal (29) at various temperatures as low as 4.2°K. At 20°K several a_g fundamentals were resolved in the mixed crystals of naphthalene and phenanthrene both in absorption and in fluorescence spectra (30). In a rigid solution of n-heptane at 77°K Bolotnikova also resolved many frequencies (28). Some Raman (31) and IR (32) (33) data are available for anthracene. In table 3 the available data concerning a_g and b_{3g} fundamentals in the $^1A_g^-$ and $^1B_{1u}^+$ electronic states are summarized.

The aim of the present experimental investigation is to analyse the vibrational and electronic states of the molecule in the 3800 Å region and to search for the origin of $^1B_{2u}^- \leftarrow {}^1A_g$ transition with its associated vibrational structure.

Table 3

a_g and b_{3g} Fundamentals Observed in Anthracene

data from absorption spectra						Data from Raman spectra (31)		
anthracene pure crystal 4.2°K (29)	anthracene in naphthalene 200K (30)	anthracene in phenanthrene 200K (30)	anthracene in MeOH-EtOH 90°K (27)	anthracene in n-heptane 77°K (28)		anthracene pure crystal	anthracene solution	
						397 cm^{-1}	400 cm^{-1}	b_{3g}
						475	474	a_g
						522	522	-
						606		"
						655	652	b_{3g}
						749(?)	745(?)	a_g
						1009	1012	b_{3g}
						1165		a_g
						1180		b_{3g}
						1261(?)	1262(?)	a_g
						1403	1397	a_g
						1413		"
						1439	1444	b_{3g}
						1481	1481	"
						1555	1551	a_g
						1632	1631	b_{3g}
350 cm^{-1}	399 cm^{-1}	393 cm^{-1}	400 cm^{-1}		a_g			
		739			"			
$^1B_{1u}^+$		1031			"			
1170	1164	1159			"			
1400	1401	1389	1450		"			
415	403			390	a_g			
757	752							
$^1A_g^-$ 1163	1165			1165	a_g			
1264	1264			1265	a_g			
1407	1416			1407				
1559	1567			1567	a_g			
				1645				

EXPERIMENTAL ARRANGEMENT

Preparation of the Samples

Scintillation grade anthracene obtained from Reilly Tar and Chemical Corporation was subjected to fourteen passes in a Fisher zone refiner. Solutions of the purified anthracene with concentrations ranging from 0.73×10^{-3}M to 5.0×10^{-4}M were prepared in spectroquality n-heptane and n-hexane supplied by Matheson Coleman & Bell. All solutions were stored in darkness to avoid photo-oxidation of anthracene.

Mixed crystals of anthracene in fluorene and in biphenyl were grown in an evacuated pyrex tube using a Bridgeman furnace (34). Eastman red label biphenyl was used without further purification. The anthracene impurity contained in a solution of Eastman red label fluorene dissolved in petroleum ether was extracted into concentrated sulfuric acid. The extraction procedure was repeated until the sulfuric acid layer remained colourless (about twelve times). The purified fluorene was recovered and was passed forty-six times through a zone refiner. Ingots about 10 cm long and 0.8 cm diameter were grown over a period of about 24 hours in a Bridgeman furnace. Monocrystalline portions of the ingots were isolated using a polarizing microscope. Selection of a single crystal sample was made after checking for

complete extinction in orthoscopic projection under a Leitz-Wetzlar polarizing microscope. The desired crystal face was found after locating the crystal axes under conoscopic examination. The chosen samples were chopped up along cleavage planes using thin razor blades, and polished by hand to the required thickness first on fine emery-paper and then on Kleenex tissues or lens tissues soaked in ethanol water mixture (1:1). The crystal thickness and the concentration of anthracene were adjusted so that the optical density of the 389 cm^{-1} a_g fundamental mode in $\underline{b}$ polarization was about 0.5 - 1.5 at room temperature. This range of the optical density was chosen to detect the various lines of different intensity. The concentrations of the mixed crystals were 0.993 - 8.00 x 10^{-4}M/M and the full thickness range available (about 0.2 mm to 2 mm) was used. The thinner crystals were prepared by mounting a larger single crystal with correct axis alignment in a brass ring packed with plaster of Paris. The samples were carefully ground and polished after the plaster of Paris had set. Before the final polish the packing around the thin crystal protected it from breakage. This method produced crystals of about the same thickness as the ring. Large single crystals of fluorene were easier to grow than biphenyl crystals.

Measurement of the Spectra

Apparatus

It was important to work at a sufficiently low temperature to resolve the vibrational structure. Liquid helium (4.2°K) and liquid nitrogen (63°K and 77°K) were used as refrigerants.

The biggest problem in taking spectra at low temperature is to ensure good thermal contact between sample and refrigerant. Some liquid cements or nail polish (35) have been recommended for this purpose. Silicone grease, rubber cement (36), nail polish and GE 7031 cement were used in the work at 4.2°K. GE 7031 cement gave the best results since the lines were sharpest (width 4 cm^{-1} for an average line in n-heptane). For the work at 4.2°K the crystal was attached to a copper disc with GE cement and the disc was secured firmly to the inner helium can. The brass solution cell (Figure 1) for n-heptane and n-hexane were attached with bolts and GE 7031 cement to ensure a good thermal contact between the cell holder and copper helium can.

The n-heptane and n-hexane solutions were also studied at liquid nitrogen temperatures using the cells shown in Figure 1. The solution was syringed into the cell through a small hole that was later sealed with a small lead ball held under pressure against the opening by a spring strip. The two quartz windows were sealed with indium O-rings.

Temperatures lower than 77°K were obtained by pumping on the liquid nitrogen, the temperature being estimated by measuring the nitrogen vapour pressure. The temperature was reduced in this way to about 63°K, the triple point of nitrogen, and this temperature was maintained for about 50 minutes before the nitrogen was completely pumped off.

Some spectra at 77°K were obtained using the apparatus shown in Figure 1. The sample was placed in the spade-shaped inner silica cell and frozen by immersion in liquid nitrogen. Resistance wire was wound in a coarse spiral around a silica dewar to avoid frosting. In this arrangement the light had to traverse both the polycrystalline sample and the liquid nitrogen around the cell.

Measurement of the Lines

All low temperature spectra in this thesis were obtained using a Hilger and Watts E 201 large Littrow spectrograph. The source for absorption and emission spectra was a high pressure Xenon lamp (Osram XBO 162). Kodak 103 a-0, 103-F and III-F spectroscopic plates were subjected to a wide range of exporsures to bring out all the lines in optimum contrast and were processed in the manner recommended by the manufacturers.

The plates were enlarged by a factor of about ten on to high contrast photographic paper (Ilford Bromide - B 3 26 K and Kodabromide A5) and the spectral lines were measured from

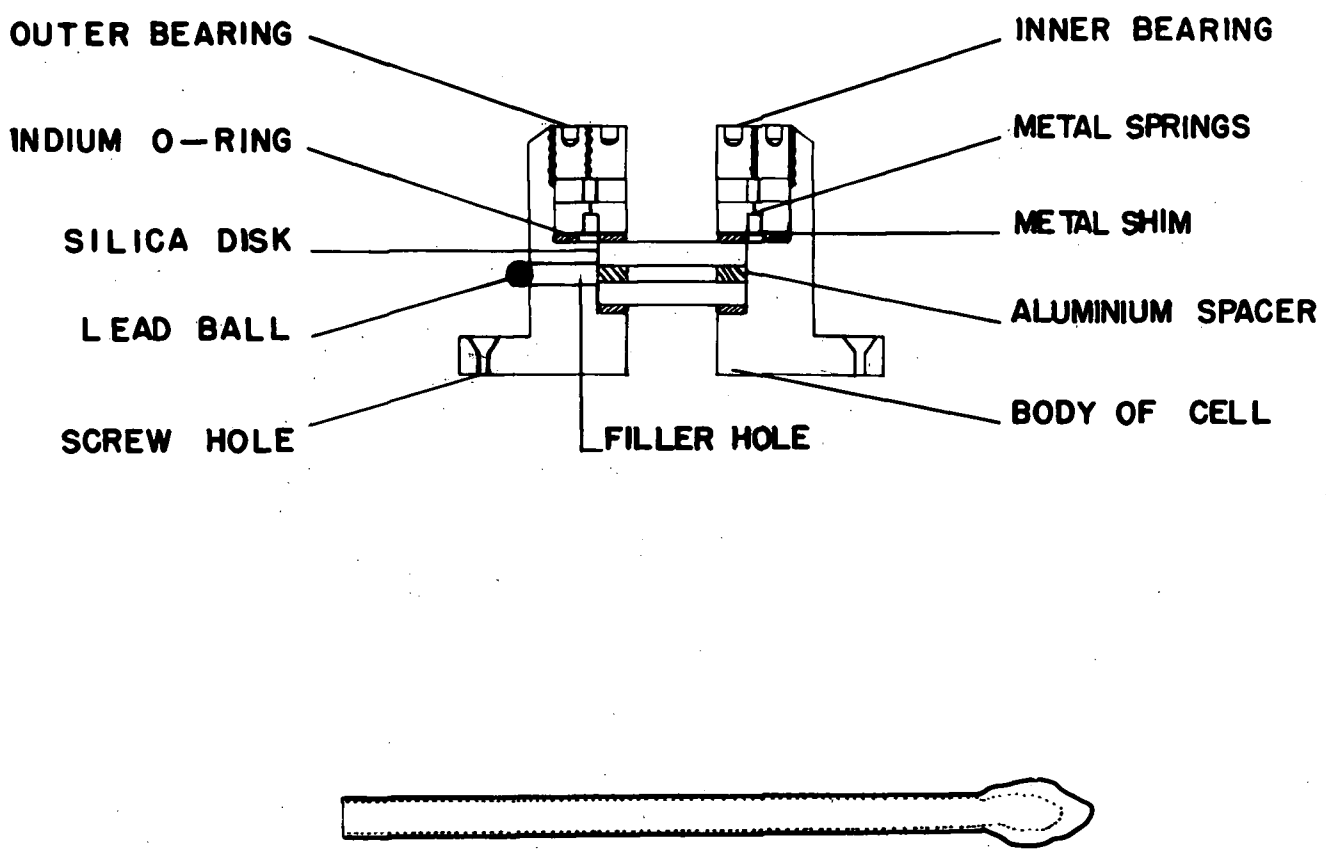

FIG 1 LOW TEMPERATURE SAMPLE CELLS

the prints by interpolation or extrapolation using nearby iron standard lines (37). Distances between lines were measured to an accuracy of about 0.1 mm by means of a precisely engraved ruler or a travelling microscope. An error of about 1 cm^{-1} was introduced by these measuring methods for even the sharpest lines. Kayser's table (38) was used to convert the wavelengths in air to the wave numbers in vacuum.

RESULTS

In Figures 2 to 7, original prints used for line measurement and sketches roughly indicating the relative line intensity are shown both in n-heptane (4.2°K) and in fluorene matrices. More precise energy values are tabulated in Tables 4 and 5 for the fluorescence and absorption spectra, respectively. The numbering in the figures correlate with those in the tables, separately for the fluorescence and absorption data. Some dotted lines in Figure 4 indicate spectral lines which were found only in special samples and whose intensities relative to other lines are not known. Not all the impurity lines for the fluorene matrix are shown; these extra lines probably arise from fluorene itself and/or some impurity such as carbazole or phenanthrene. Table 6 shows absorption lines arising from the fluorene matrix at 4.2°K.

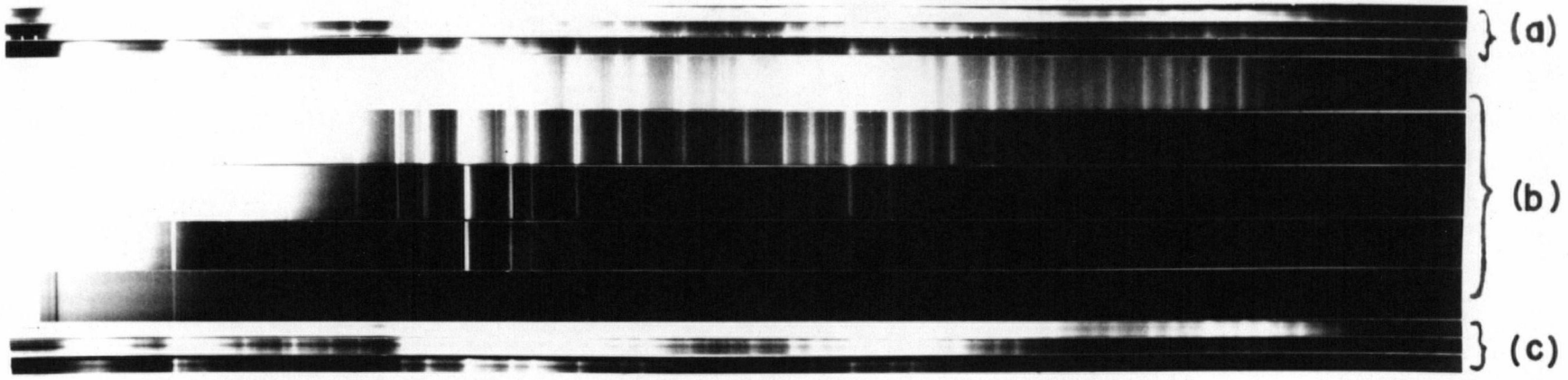

(a) fluorene ∥b(M)

(b) n-heptane

(c) fluorene ∥c(L)

FIGS 2 AND 3 THE FLUORESCENCE SPECTRA OF ANTHRACENE IN n-HEPTANE AND FLUORENE AT 4.2°K

(a) Anthracene in n-heptane at 4.2°K

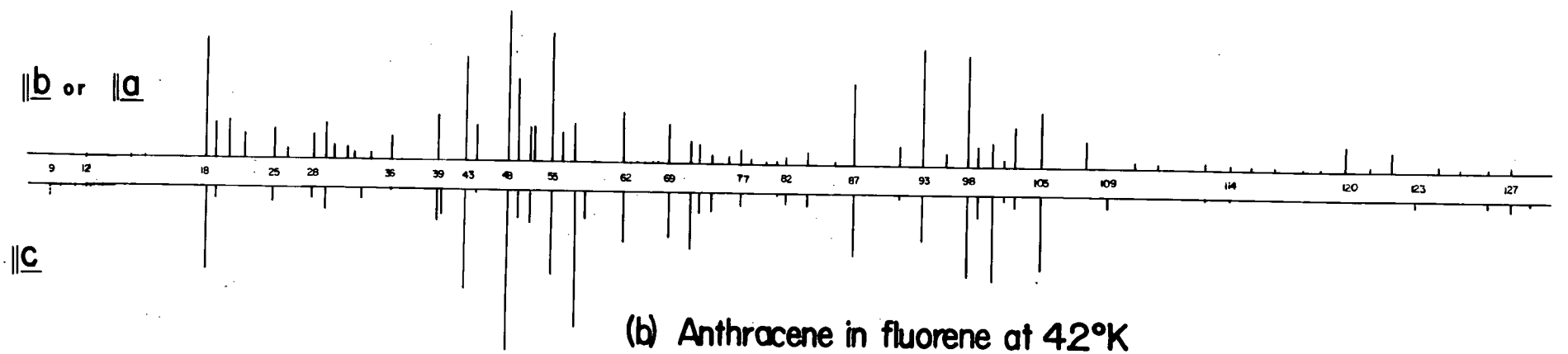

(b) Anthracene in fluorene at 42°K

FIG 4 RELATIVE INTENSITIES OF THE LINES IN FLUORESCENCE

Table 4

Fluorescence Spectra of Anthracene in Various Matrices

	biphenyl, a. 4.2°K n-hexane 77°K			Fluorene, 4.2°K		n-heptane		remarks b.
	11M (b)	11L (c)		11M (b,a)	11L (c)	63,77°K	4.2°K	
1				-2744	-2744			
2				-2446	-2446			
3				-2154	-2154			
4				-1814	-1814			
5				-1600	-1600			
6				- 809	- 809			
7				- 282	- 282			
8				- 226	- 226			
9					- 164		- 166	
10					- 131			
11					- 46			
12	26056	26056	26498	25975	25975	26247	26211	0-0, origin[c]
13					16			
14					51			
15	136	136		148			179	
16	184	184		196			214	
17							368	394-25
18	406	406		396	398	398	394	394, ag
19				429				
20	466	466		471				
21	532	532		527			510	510, ag?
22							553	impurity
23							575	
24							589	
25	620	620		621	625	627	629	629, ag
26	675	675		670	670			
27							734	
28	754	754		755	755	763	759	759, ag
29							778	
30	795	795	794	794	792	792	787	2x394-1
31				828				
32	880	880		870			874	
33				894				
34		905			917		911	911, b3g
35	962	962		950				
36	1025	1025		1019	1022	1021	1020	1020, ag
37					1052	1044	1045	1045, b3g?
38				1130			1141	394+759-12, FR[d]
39	1173	1173	1177	1175	1175	1169	1163	1163, ag

Table 4 continued

	biphenyl, a. 4.2°K 11M (b)	11L (c)	n-hexane 77°K	Fluorene, 11M (b,a)	4.2°K 11L (c)	n-heptane 63,77°K	4.2°K	remarks b.
40		1193			1186	1194	1180	1180, b3g
41							1233	2x616 (b2u) + 1?
42							1257	2x629-1,FR
43	1244	1244	1272	1268	1268	1267	1267	1267, ag
44							1283	
45		1269		1305	1305		1305	394+911
46				1356	1356		1340	
47							1383	1409-25-1
48	1414	1414	1415	1411	1411	1413	1409	1409, ag
49	1454	1454		1442	1442		1431	629+2x394 +14,FR
50				1484	1484			
51				1501				?e
52	1516	1516					1516	2x759-2
53							1538	1568-25-5
54							1652	394+1163+5
55	1559	1559	1567	1562	1562	1568	1568	1568, ag
56	1620	1620		1598	1597			
57			1699	1640	1640	1643	1639	1639, b3g
58					1675		1660	1660, b3g
59					1706		1715	2x394+911-16
60							1736	
61							1781	629+1163-10; 759+1020+2; 394+1409-25 +3
62	1810	1810	1809	1806	1806	1808	1803	394+1409
63				1826				?
64				1848				
65	1877	1877		1877				
66							1888	629+1267-8
67				1906			1910	394+2x759-2
68				1922			1924	759+1163-2
69	1962	1962	1963	1957	1957	1963	1960	394+1568-2
70							1996	?
71	2039	2039	2037	2030	2030	2037	2033	394+1639
72				2061	2061		2049	394+1660-5
73							2072	510+1568-6,?
74					2100			
75							2124	
76				2160			2163	759+1409-5

Table 4 continued

	biphenyl, a. 4.2°K 11M (b)	11L (c)	n-hexane 77°K	Fluorene, 11M (b,a)	4.2°K 11L (c)	n-heptane 63,77°K	4.2°K	remarks b.
77	2202	2202		2193	2198	2204	2195	2x394+1409-2
78				2237				
79							2270	629x1639+2
80				2286			2290	1020+1267+3
81				2322			2329	759+1568; 2x1163+3
82	2340	2340		2352	2354		2358	2x394+1568+2
83							2399	759+1639+1
84	2435	2435		2427	2427	2435	2426	1020+1409-3
85							2502	
86				2523	2523		2523	2x1267-11
87	2587	2587	2577	2580	2580	2572	2571	1163+1409-1
88					2594		2591	1180+1409+2
89							2637	1020+1639-22
90	2681	2681	2671			2677	2669	1267+1409-7
91				2737	2729		2730	1163+1568-1
92		2819					2753	1180+1568+5
93	2828	2828	2821	2815	2815	2819	2818	2x1409
94							2831	1267+1568-4
95	2906	2906		2897	2897		2894	1267+1639-12
96							2905	
97							2923	1267+1660-4; 2x759+1409-4 394+2x1267-5
98	2978	2978	2967	2966	2965	2973	2969	1409+1568-8; 394+1163+ 1409+3
99				2999	2999			
100	3047	3047		3050	3050	3041	3043	1409+1639-5
101							3064	394+1267+ 1409-3
102				3084	3084		3090	3090, ag?
103	3122	3122		3131	3131	3136	3129	2x1568-7
104		3220			3199			1568+1639
105	3205			3211		3212	3208	394+2x1409-4
106	3273	3273					3271	2x1639-7
107		3303					3301	629+1267+ 1409-4
108	3359	3359				3365	3363	394+1409+ 1568-8; 2x394+1163+ 1409+3
109	3425	3425		3434	3440	3450	3438	629+2x1409-9; 394+1409+ 1639+4

Table 4 continued

	biphenyl, a. 4.2°K 11M (b)	11L (c)	n-hexane 77°K	Fluorene 11M (b,a)	4.2°K 11L (c)	n-heptane 63,77°K	4.2°K	remarks b.
110	3492	3492		3521			3526	
111	3579	3579		3598	3598		3596	2x394+2x1409-11; 629+1409+1568-11; 2x394+1163+1409+4
112							3732	759+1409+1568-4; 911+2x1409+3394+759+1163+1409+9
113	3778			3756	3758		3754	2x394+1409+1568-13
114	3841			3838	3838		3833	1020+2x1409-5
115	3935			3912				
116	3992			3984			3978	1163+2x1409-3,?; 1020+1409+1568-19
117	4087			4080			4075	1267+2x1409-6
118							4125	394+1409+2x1163-4
119	4164			4138			4154	
120	4246			4222		4228	4224	3x1409-3
121				4301			4297	
122	4398			4372		4379	4372	1568+2x1409-14
123					4450		4449	1639+2x1409-8
124				4524	4524		4524	1409+2x1568-21
125				4600			4605	394+3x1409-16
126				4692	4681		4696	394+1267+1409+1639+7
127				4765	4757		4767	394+1568+2x1409-13; 2x1568+1639-8 2x394+1163+2x1409-2
128				4832				

Table 4 continued

a. Crystal axes are shown in brackets while M and L show molecular short and long axes, respectively.

b. Assignments are made using the data from the n-heptane spectrum.

c. The origins in the different matrices are given in cm^{-1}, and all the other entries in the table show differences from the origin.

d. (FR) Fermi resonance.

e. Doubtful in its appearance.

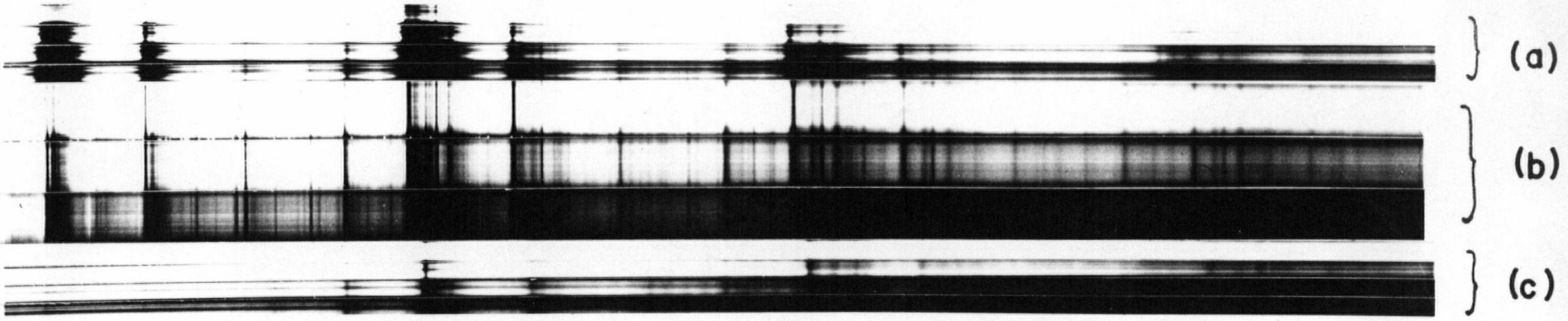

(a) fluorene || b (M)

(b) n-heptane

(c) fluorene || c (L)

FIGS 5 AND 6 THE ABSORPTION SPECTRA OF ANTHRACENE IN n-HEPTANE AND FLUORENE AT 4.2 °K

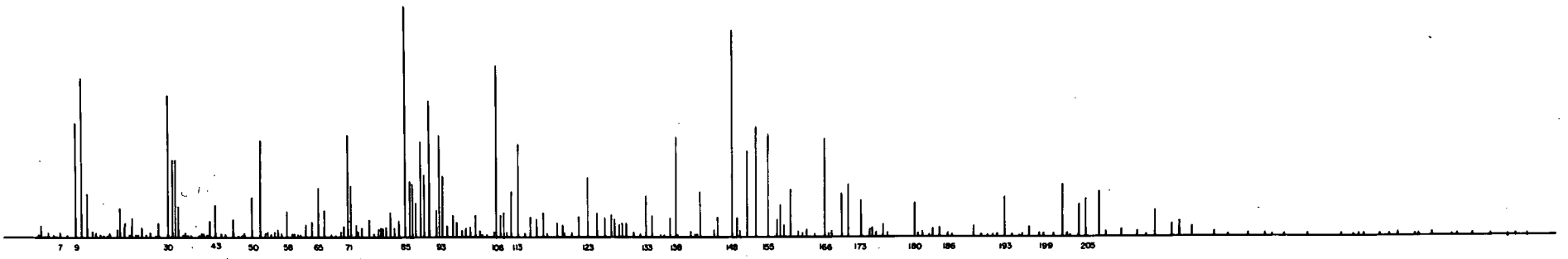

(a) Anthracene in n-heptane at 4.2°K

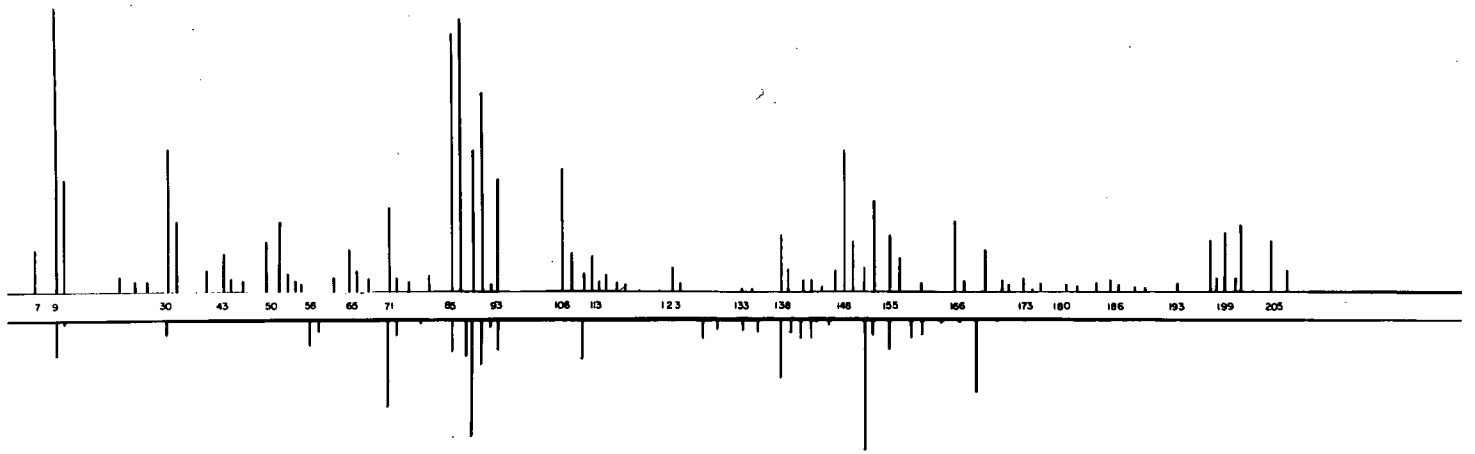

∥b or ∥a

∥c

(b) Anthracene in fluorene at 4.2°K

FIG 7 RELATIVE INTENSITIES OF THE LINES IN ABSORPTION

Table 5

Absorption Spectra of Anthracene in Various Matrices

	biphenyl a. 4.2°K		n-hexane	fluorene, 4.2°K		n-heptane			remarks [b]
	11M (b)	11L (c)	77°K	11M (b,a)	11L (c)	77°K	63°K	4.2°K	
1								-154	
2			-136					-144	
3								-127	
4								-112	
5								- 92	
6								- 80	
7				-73				- 73	
8								- 43	
9	26056		26498	25975		26247	26239	26221	0-0, origin[c]
10				29		24	24	25	25, lattice
11								47	2x25-3?; 47?
12								70	
13								85	
14								105	
15								118	
16								133	
17								146	
18								178	
19								187	
20				219				211	
21								229	
22								236	
23			253					254	
24								262	
25				273				279	
26								299	
27				317				316	
28								340	
29								351	
30	391	385	389	392	385	387	389	389	389, ag
31				422				410	389+25-4
32								420	2x211-2 FR[d]?
33								436	389+2x25-3?
34								457	
35								464	
36								474	
37								484	
38				523				521	
39								531	
40								539	
41								553	
42								566	
43	583		581	585		590	589	590	590, ag

Table 5 continued

	biphenyl a. 4.2°K 11M (b)	11L (c)	n-hexane 77°K	fluorene, 4.2°K 11M (b,a)	11L (c)	n-heptane 77°K	63°K	4.2°K	remarks b.
44				610				616	590+25+1
45								628	
46				652			658	663	663, ag?
47								687	
48								703	
49								709	
50	735		729	733		740	740	744	744. ag
51	778		773	780		777	780	779	2x389+1
52				812				798	2x389+25-5
53								809	389+2x211-2 FR?
54								823	
55				836				840	
56				859				857	
57								871	
58			882		891	890	892	894	894,b3g
59								918	
60					927			926	
61								941	
62								955	
63				977				979	389+590
64								1005	2x211-7 FR?
65	1024		1023	1028		1024	1027	1030	1030, ag
66				1055		1055	1062	1057	389+663+5, FR?
67								1084	
68				1096				1102	
69								1126	
70							1143	1135	389+744+2
71	1158		1152	1169		1155	1160	1157	1157, ag
72					1166			1166	1166, b3g
73								1190	
74				1199	1199			1199	11L:1166+24+9
75								1213	
76				1239				1247	1247, ag?
77								1266	
78					1285			1283	389+894
79				1311				1297	
80								1304	
81							1327	1318	2x663-8?
82								1338	590+744+4, FR?
83								1354	
84								1374	590+2x389+6, FR
85	1391		1386	1396		1396	1397	1399	1399, ag
86				1422				1418	389+1030-1, FR

Table 5 continued

	biphenyl a. 4.2°K		n-hexane	fluorene, 4.2°K		n-heptane			
	11M (b)	11L (c)	77°K	11M (b,a)	11L (c)	77°K	63°K	4.2°K	remarks b.
87							1427	1431	1399+25+7, FR
88					1443			1447	
89				1467	1462	1458	1463	1464	11L:1464, b3g
90					1495		1482	1480	590+894-4, FR
91	1496		1491	1498		1498	1504	1503	1503, ag
92				1532				1533	744+2x389+11, FR; 1503+25+5
93	1541		1554	1555		1547	1551	1547	389+1157+1
94					1560			1559	389+1166+4
95								1578	389+1157+25+7
96							1601	1604	
97								1619	590+1030-1
98								1641	389+1247+5?
99								1658	
100						1591	1699	1700	663+1030+7?
101								1720	389+2x663+5?
102								1727	
103								1749	590+1157+2
104								1785	2x894-3
105			1779	1783		1786	1789	1788	389+1399
106								1809	2x389+1030+1; 389+1399+25-4
107				1814				1822	663+1157+2, FR?
108								1834	663+3x389+4?
109				1860	1853	1853	1860	1855	389+1464+2
110	1890		1880	1892		1887	1893	1885	389+1503-7
111				1917				1917	
112	1935		1932	1941				1936	2x389+1157+1
113						1959	1971	1963	
114	1979			1978		1986	1990	1993	590+1399+4
115				2006				2008	
116	2048		2035	2056		2052	2051	2051	2x1030-9
117							2094	2071	663+1399+9?
118								2112	2x389+2x663+8?
119	2128					2145	2141	2141	744+1399-2
120	2178		2171	2176		1177	2181	2178	2x389+1399+1
121				2202					
122						2220	2225	2220	389+663+1157+6
123	2243					2248	2256	2254	744+1503+7
124						2287	2287	2285	2x389+1503+4
125			2276		2286			2296	894+1399+3
126	2322		2321					2319	2x1157+5
127					2336	2336	2331	2329	1157+1166+6

Table 5 continued

	biphenyl a. 4.2°K		n-hexane	fluorene, 4.2°K			n-heptane		
	11M (b)	11L (c)	77°K	11M (b,a)	11L (c)	77°K	63°K	4.2°K	remarks
128							2348	2347	
129								2378	389+590+1399
130								2404	1157+1247?; 894+1503+7?
131		2416		2422	2425	2426	2428	2428	11M:1030+1399-1?
132				2555		2449	2458	2457	389+663+1399+6?
133	2481				2482			2490	1030+1464-4
134								2508	389+663+1464-8?
135								2533	1030+1503
136	2560		2548	2561	2561	2560	2562	2559	11M:1157+1399+3; 11L:1166+1399
137					2623	2607	2617	2620	1157+1464-1
138				2637	2637			2638	11M:389+744+1503+2; 11L:3x389+1464-7?
139								2648	1247+1399+2?
140			2650	2665	2668	2655	2665	2660	11M:1503+1157 11L:1503+1167+1
141	2710		2715	2701					
142					2729			2720	389+1157+1166+8
143				2751					
144						2728	2730	2734	590+744+1399+2, FR
145				2783		2796	2800	2798	2x1399
146				2816				2818	389+1030+1399; 2x1399+25-5
147								2832	663+2x389+1399+8?; 2x389+894+1157+4?
148					2855	2861	2863	2864	1399+1464+1
149	2893		2886	2890		2897	2901	2900	1399+1503-2
150	2941		2947	2945	2945	2947	2955	2954	11L:1464+1503-11; 11M:389+1399+1157+7
151	2964			2978				2954	2x744+1503, FR
152	3007						3010	3004	2x1503-2
153					3022			3020	389+1157+1464+10
154	3039			3053	3057		3052	3048	11M:389+1157+1503+1 11L:389+1166+1503-1
155								3081	3x1030-9; 2x389+2x1157-11
156								3100	2x389+1157+1166-1
157					3126			3119	C-H stretch, b3g?
158								3152	590+1157+1399+6
159	3174		3178	3176	3191	3187	3189	3193	11M:389+2x1399+6 11L:389+590+744+1464+6
160								3212	2x389+1030+1399+5

Table 5 continued

	biphenyl a. 4.2°K		n-hexane	fluorene, 4.2°K		n-heptane			
	11M (b)	11L (c)	77°K	11M (b,a)	11L (c)	77°K	63°K	4.2°K	remarks
161								3227	389+590+744+1503+1
162					3248	3254	3258	3264	389+1399+1464+12
163	3283		3277	3280		3288	3292	3293	389+1399+1503+2
164	3333		3339	3340		3342	3345	3348	2x389+1164+1399+7?
165				3365			3389	3384	590+2x1399-4
166								3394	389+2x1503-1
167				3416				3414	744+1157+1503+7
168			3433	3443		3446	3439	3442	2x389+1157+1503+4
169				3476				3460	1399+2x1030+1
170	3565		3569	3564		3573	3580	3574	2x389+2x1399-3
171								3588	1030+1157+1399+2
172				3602				3609	590+2x1503+13
173								3634	e
174				3668			3654	3648	744+1399+1503+2
175			3666			3678	3688	3678	2x398+1399+1503
176			3718	3718				3714	1399+2x1157+1
177				3750		3723	3737	3731	3x389+1157+1399+8
178			3813	3804		3823	3823	3826	1030+2x1399-2; 1503+2x1157+9?
179				3838		3858	3857	3853	389+663+2x1399+3?
180								3886	1030+1399+1464-7?
181								3903	1157+1247+1503-4? 894+2x1503+3?
182								3922	1030+1399+1503-10; 389+744+2x1399-9?
183	3955		3944	3948			3968	3955	1157+2x1399
184								3985	389+1030+1166+1399+1; 389+1030+1157+1399+10
185						4013		4017	1157+1399+1464-3
186							4035	4030	1030+2x1503-6
187			4042	4066		4058	4073	4055	1157+1399+1503-4
188				4097			4112	4100	389+1399+2x1157-2
189			4108	4117		4118	4134	4118	1157+1464+1503-6
190				4149				4160	1157+2x1503-1
191	4177		4180	4172		4197	4199	4195	3x1399-2
192				4198				4214	389+1030+2x1399-3; 389+2x1157+1503+8
193								4227	663+2x389+2x1399-12?
194					4225	4262	4261	4265	1464+2x1399+3
195	4280		4278	4280		4294	4301	4297	1503+2x1399-4
196	4328		4339	4327		4349	4352	4351	389+1157+2x1399-7
197					4368				392+1166+2x1396+18
198					4388			4380	1399+1464+1503+14

Table 5 continued

	biphenyl a. 4.2°K		n-hexane	fluorene, 4.2°K		n-heptane			
	11M (b)	11L (c)	77°K	11M (b,a)	11L (c)	77°K	63°K	4.2°K	remarks
199			4433	4438			4447	4446	389+1157+1399+1503+2; 389+1166+1399+1503-7?
200				4515			4513	4509	3x1503
201				4552				4545	389+1157+2x1503-7
202			4572	4582		4585	4589	4584	389+3x1399-2
203				4630	4630	4699	4656	4655	389+1464+2x1399+4
204			4668	4667		4684	4691	4683	389+1503+2x1399-7
205			4723	4700		4739	4741	4739	2x389+1157+2x1399+6; 2x389+1166+2x1399-3
206				4829				4832	2x389+1157+1399+1503-5
207								4890	389+3x1503-8; 590+1503+2x1399-1
208								4973	2x389+3x1399-2
209								5047	2x389+1464+2x1399+7; 744+1503+2x1399+2
210								5076	2x389+1503+2x1399-3
211								5126	2x1157+2x1399+14?; 1157+1166+2x1399+5
212								5227	1030+3x1399; 1030+1503+2x1399-4; 1399+1503+2x1157+11? 1157+1166+1399+1503+2?
213								5366	1157+3x1399+12; 1166+3x1399+3
214								5417	1157+1464+2x1399-2;
215								5437	1247+3x1399+7?
216								5458	1157+1503+2x1399
217								5522	1157+1399+1464+1503-1
218								5567	1464+3x1399+6; 1157+1399+2x1503+5?
219								5596	4x1399
220								5672	1157+3x1503+6; 1464+3x1399+11
221								5684	1503+3x1399-16
222								5741	389+1157+3x1399-2; 389+1166+3x1399-11?
223								5825	389+1166+1464+2x1399+8 389+1157+1464+2x1399+17
224								5846	389+1157+1503+2x1399-1
225								5910	1399+3x1503+2
226								5983	389+4x1399-3
227								6053	389+3x1399+1464+3

Table 5 continued

biphenyl (a., 4.2°K 11M (b)	11L (c)	n-hexane 77°K	fluorene, 4.2°K 11M (b,a)	11L (c)	n-heptane 77°K	63°K	4.2°K	remarks
228							6084	389+1503+3x1399-5
229							6135	2x389+1157+3x1399+3; 2x389+1166+3x1399-6

a. Crystal axes are shown in brackets while M and L show molecular short and long axes, respectively.

b. Assignments are made using the data from the n-heptane spectrum.

c. The origins in the different matrices are given in cm^{-1}, and all the other entries in the table show differences from the origin.

d. (FR) Fermi resonance.

e. This line is doubtful.

Table 6

Absorption Spectrum of Fluorene at 4.20K [a.]

	11M (b)[b.]	11L (c)		11M (b)	11L (c)		11M (b)	11L (c)
1		31062	35	31665		69	32219	
2		31080	36	31666	31668	70		32230
3		31130	37	31695	31696	71	32246	
4		31141	38	31716		72	32254	
5		31157	39		31738	73		32262
6	31182		40	31742		74	32274	
7		31190	41		31750	75	32298	
8		31211	42	31795		76	32319	
9		31230	43	31809		77		32323
10	31256	31255	44		31813	78		32359
11		31264	45		31835	79	32367	
12	31290	31290	46		31844	80	32381	
13		31299	47	31857	31857	81		32385
14	31318	31319	48	31863	31860	82	32394	
15		31350	49		31892	83		32398
16	31363		50		31902	84	32420	
17	31377	31379	51	31919		85	32433	
18	31409	31410	52		31928	86	32455	32455
19		31417	53		31956	87	32481	32480
20	31439		54	31959	31961	88	32494	
21		31473	55		31967	89	32502	
22		31478	56	31984		90	32526	
23		31499	57		31992	91	32543	
24		31512	58	32005	32001	92	32569	
25	31517		59		32017	93	32590	
26	31520		60		32049	94	32603	
27	31524	31524	61	32066		95	32619	
28	31550	31548	62	32086	32082	96	32644	
29		31584	63	32109	32110	97	32672	
30		31651	64	32130		98	32687	
31	31619		65	32148		99	32706	
32		31623	66	32154		100	32731	
33		31636	67		32161	101	32752	32755
34		31656	68	32206	32203	102	32761	
103		32766	105	32805		107	32829	
104	32787		106	32815		108	32858	

a. The frequency of each line is given in cm^{-1}.

b. Crystal axes are shown in brackets while M and L show molecular short and long axes, respectively.

DISCUSSION

Fluorescence Spectra

Fundamental Modes

Spectral lines in fluorescence may arise from anthracene molecules, molecules of the matrix or some other impurity molecule. Unknown impurities present a real problem in fluorescence spectroscopy since a very small trace of impurity (as low as 10^{-6}M) can make a large contribution to the overall emission.

Lines due to fundamental modes of anthracene may be distinguished from other emission lines since only these form combinations built on the origin and the origin can be assigned from the absorption spectrum. On the basis of their intensities, polarization and ability to form combinations eight a_g fundamental modes of the ^1A_g electronic state were assigned: 394, 629, 759, 1020, 1163, 1267, 1409 and 1568 cm^{-1}. Theoretically twelve a_g fundamentals are predicted for anthracene and among them three due to C-H stretches appear in the region of 2900 - 3100 cm^{-1} (39). So below 2000 cm^{-1} nine a_g modes should be found. From their intensity and polarization behaviour either 510, 874 or 1340 cm^{-1} may be selected as this ninth a_g fundamental. Among these 510 and 1340 cm^{-1} modes appeared one and four times respectively

in combination with known a_g modes while 874 cm^{-1} did not appear at all. From this point of view, the ninth fundamental is most probably the line at 1340 cm^{-1} with the line at 510 cm^{-1} preferred next. However, 1340 cm^{-1} did not appear in biphenyl while the other two did. Further, Raman data (31) shows 522 cm^{-1} as a_g in anthracene crystal and in solution which is probably close enough to our 510 cm^{-1}. No lines corresponding to the other two vibrations were found in the Raman. Thus although no definite assignment could be made for the ninth a_g fundamental, the line at 510 cm^{-1} seems to be the most probable contender if emphasis is placed on its appearance in the Raman spectra. The other two must be interpreted as impurity lines or b_{3g} belonging to the electronic state if for some reason fluorescence appears from a $^1B_{2u}$ origin. 3090 cm^{-1} may be assigned as an fundamental due to C-H stretching since it does not analyse as a combination line, it agrees with previous empirical data (39) and it has the expected polarization. However, 3526 cm^{-1} is probably too high to be assigned as an a_g C-H stretching frequency.

Five b_{3g} fundamentals were found for the ^1A_g electronic ground state at 911, 1045, 1180, 1639 and 1660 cm^{-1}. They were usually weaker in intensity than the a_g modes and so detection of combinations was difficult. However, combinations involving all modes except 1045 cm^{-1} were found. The b_{3g} assignment rests primarily on polarization data (i.e., all these lines appeared more strongly in the c direction of

the fluorene matrix). The modes at 1180 and 1639 cm^{-1} agreed closely with Raman data (31). Although the 1045 cm^{-1} mode did not combine with other fundamentals, it is tentatively assigned as a b_{3g} fundamental since it is close to the 1012 cm^{-1} b_{3g} fundamental observed in the Raman spectrum (31).

Fermi Resonance

Three possible examples of Fermi resonance were observed in fluorescence (Table 7). All of these occured near strong a_g fundamentals as expected. In set (a) energy shifts of those two lines were found, in set (b) intensity transfer was more significant, while in set (c) both intensity and energy were affected strongly.

Table 7

Possible Examples of Fermi Resonance in the Fluorescence of Anthracene

set	line No.	in n-heptane	in fluorene	in biphenyl
(a)	38	1141=394+759-12	1130=396+755-21	
	39	1163 ag	1175 ag	
(b)	42	1257=2x629-1		
	43	1267 ag		
(c)	48	1409 ag	1411 ag	1414 ag
	49	1431=2x391+629+14	1442=2x396+621+29	1454=2x406+620+22

Other Features

If errors of measurement due to line broadening (see lines 59, 86 and 95) are taken into account, the combinations suggest the usual diatomic type of potential curve, which is anharmonic in high quantum region. Combinations of four fundamentals represented the most complex lines observed in our spectra and these were perhaps beginning to show anharmonicity of the ^1A_g potential surface. However, the potential surface was surprisingly harmonic for such a large polyatomic molecule.

The origin and the 25 cm^{-1} lattice mode built on the origin did not appear in fluorescence and this can be explained in terms of reabsorption of the emission. Both of these lines appeared strongly in absorption.

Theoretically, fundamental modes of any symmetry species may combine provided that the combination has the symmetry a_g or b_{3g}. In practice, combinations of this general type do not appear. However, line 41 at 1233 cm^{-1} might be interpreted as the overtone of the b_{2u} mode at 616 cm^{-1} observed in the infra-red (32); no combination of the observed a_g and b_{3g} can account for this line, although the possibility of arising from impurity must be considered.

Some lines appeared, which could not be assigned in terms of the observed a_g and b_{3g} fundamentals. These may be separated into two kinds: (i) lines which appeared in only one of the four matrices, and (ii) lines which appeared in

more than one matrix.

The lines belonging to (i) may arise from impurities in the matrix or from the host molecule. Further if we assume a "solvent" shift of the $^1B_{2u} \leftarrow {}^1A_g$ origin different from that of the $^1B_{1u} \leftarrow {}^1A_g$ origin, then the unexplained lines could be interpreted as ground state vibrational modes from a $^1B_{2u}$ upper electronic state. Phenanthrene, carbazole and acridine are possible impurities in the matrices, fluorene and biphenyl because they are isomorphic with those impurities.[40] Phenanthrene (41) (42) and carbazole (43) fluoresce near the origin of anthracene. Since acridine does not fluoresce in its crystal state or in organic solvent (44) at least at room temperature and since its fluorescence spectrum is to the red of the anthracene spectrum (44), the presence of acridine is not important in the analysis of fluorescence. In general if a line appears only in a special matrix and if the intensity relative to the other common lines differs over a number of samples, it may be taken as an impurity line. In this sense only line 22 at 533 cm^{-1} apparently arose from some impurity. Since the spectra of phenanthrene and carbazole measured under the same experimental conditions as here are not available, the precise assignment of impurities is not possible at present. Fluorene fluoresces to the blue of the origin of anthracene (43) and the lines 1 and 2 probably form part of the fluorene fluorescence spectrum because they agree closely with the data taken at 77°K in n-heptane (43). Biphenyl does

not fluoresce in this region (27) and neither do n-heptane nor n-hexane. The remaining possible interpretation of the lines (i) involved a transition from a $^1B_{2u}$ upper state. If this is true, a somewhat similar intensity and energy separation to vibrational modes from the $^1B_{1u}$ system should be observed. However, this was not so and this last possibility may be excluded.

For the lines belonging to (ii) three possible interpretations may exist: impurities in anthracene, lines from the light source, and vibrational modes due to fluorescence from the $^1B_{2u}$ state assuming no "solvent" shift. As impurities in anthracen anthraquinone must be considered in addition to carbazole and phenanthrene, for the oxidation of anthracen could occur especially in the presence of light and oxygen. Anthraquinone vapour (45) fluoresces in the region 20,000 - 23,000 cm^{-1}. Thus the lines 115 and 121 could be due to anthraquinone, and the lines near the origin (9, 15, 16, 20 and 35) might arise from either carbazole or phenanthrene, but again precise assignment is impossible for the lack of data. If emission from the source appeared, the line must show the same energy independent of the matrix. From this point of view no lines arose from the common source xenon. Thus to account for the presence of the unassigned lines in the fluorescence spectra, the existence of some impurities must be claimed.

Absorption Spectra

Fundamental Modes of the $^1B_{1u}$ Upper State

From a preliminary examination of their polarization, intensity and appearance in combinations, fifteen intervals may be chosen as fundamentals with energy less than 2000 cm^{-1}; e.g. eleven a_g fundamentals: 389, 590, 744, 1030, 1157, 1399, 1503, 663, 1057, 1247 and 1338 cm^{-1}, and four b_{3g} fundamentals: 894, 1166, 1464 and 926 cm^{-1}. Since there can be only twelve a_g fundamentals in all and three are expected in the region of C-H stretching frequencies near 3000 cm^{-1} there must be only nine a_g fundamentals below 2000 cm^{-1}. The first seven a_g fundamentals and the first three b_{3g} fundamentals are assigned with certainty. Thus two more a_g fundamentals must be selected from the last four listed. The interval 3119 cm^{-1} in n-heptane might be added as a b_{3g} C-H stretching frequency.

The line at 663 cm^{-1} may be assigned as an a_g fundamental with some certainty although it did not appear in n-hexane or in biphenyl. No alternative explanation for it was possible, and many lines could be best interpreted as combinations involving 663 cm^{-1} as an a_g fundamental. The line at 1057 cm^{-1} was slightly stronger than 663 cm^{-1} and appeared in n-heptane at 77°K while 663 cm^{-1} did not. However, it was not so useful as 663 cm^{-1} in interpreting combinations and 1057 cm^{-1} could itself be interpreted as the combination (590+663) cm^{-1} especially when the possibility of Fermi resonance between

this combination and the strong a_g fundamental 1030 cm^{-1} was considered. Thus 1057 cm^{-1} was taken as a combination rather than an a_g fundamental. Both 1247 and 1338 cm^{-1} could be taken as fundamentals or as the combinations 1247 = 590+663-6 and 1338 + 590+744+4; although the lines appeared to be too intense to be simple combinations. The line at 1338 cm^{-1} was sufficiently close to the strongest line in the spectrum at 1399 cm^{-1} for its intensity as a combination to be accounted for. However, the line at 1247 cm^{-1} was more isolated from other strong lines so that, in this case, a Fermi resonance could not readily be assumed. Again the line 1247 cm^{-1} appeared in the fluorene matrix while the other did not. Thus, on these grounds, 663 and 1247 cm^{-1} are tentatively assigned as a_g fundamentals and added to the previous list of seven.

As a b_{3g} fundamental 926 cm^{-1} is quite doubtful, however the alternative explanation (894+25+7) is also doubtful, and the line at 2428 cm^{-1} could be accounted for as a combination of 926 and 1503 cm^{-1} (long axis polarized). The combination of 926 cm^{-1} with the stronger a_g fundamental at 1399 cm^{-1} could not be found since it was hidden beneath the combination 2329 = 1157+1166+6.

Comparison of the Fundamentals on the ^1A_g and on the $^1B_{1u}$ Electronic States

All possible fundamentals of anthracene in the ground and in the excited state $^1B_{1u}$ are summarized in Table 8.

For the fundamentals which have been assigned with certainty, a correspondence between each fundamental at the two electronic states have been observed both in energy value and intensity. This indicates that the potential energy surfaces of the ground and the excited electronic state are similar in these normal coordinates at least. This leads to the expectation that there will be a correspondence for all the intervals, and the two a_g fundamentals tentatively assigned (663 and 1247 cm^{-1}) might be added to the six certain ones to account for the nine a_g fundamentals as predicted.

Further there is a tendency that the fundamentals in the ^1A_g state have higher energy than those in the $^1B_{1u}$ state. This behaviour has been also observed in naphthalene (46).

Table 8

The Fundamentals of Anthracene in the ^1A_g Ground and the $^1B_{1u}$ Upper State

^1A_g	$^1B_{1u}$	Remark
cm^{-1}	cm^{-1}	
394	389	certain
510	590	probable
629	663	probable
759	744	certain
874		doubtful
1020	1030	certain
	1057	389+663+5, FR?
1163	1157	certain
1267	1247	probable
1340	1338	590+744+4:in $^1B_{1u}$ state only
1409	1399	certain
1568	1503	certain
3018		C-H stretch??
911	894	certain
1045	926	possible
1180	1166	certain
1639	1464	certain
1660		certain
	3119	C-H stretch??

Fermi Resonance

Possible examples of Fermi resonance in absorption are summarized in Table 9.

Table 9

Possible Examples of Fermi Resonance in the Absorption of Anthracene

set	line No.	in n-heptane, at 4.2°K	in fluorene, at 4.2°K
a	65	1030, ag	1028, ag
	66	1057 = 389+663+5	1062 = 387+657+18
	82	1338 = 590+744+4	
	84	1374 = 590+2x389+6	
b	85	1399, ag	1396,ag
	86	1418 = 389+1030-1	1422 = 392+1028+2
	89	1464, b3g	1462, b3g
c	90	1480 = 590+894-4	1495 = 585+891+19
	105	1788 = 389+1399	1783 = 392+1396-5
d	107	1822 = 663+1157+2	1814 = 652+1169-7
	144	2734 = 590+744+1399+2	
e	145	2798 = 2x1399	
	150	2954 = 389+1157+1399+7	2445 = 392+1169+1396-12
f	151	2991 = 2x744+1503	2978 = 2x733+1498+14

All of these examples show a more pronounced Fermi resonance in the fluorene matrix; this was the tendency in

fluorescence also. The sets in the fluorene matrix a, c and f show good examples of the effect both in terms of the energy shift and intensity transfer. The other sets in fluorene and all the sets in n-heptane show only an intensity transfer. In set b the strong a_g fundamental at 1399 cm^{-1} seems to share the intensity among several nearby combinations. However, since there must be some error in estimating intensities from the photographic prints, particularly near the strong line at 1339 cm^{-1}, actual Fermi resonance might occur only between the lines 85 and 86.

Although anharmonicity increases in the higher energy region, no Fermi resonances were identified because of the decreasing intensity of the lines with a consequent increase in the measurement error due to line broadening. In the other two matrices a lower resolution of the spectra did not allow Fermi resonance to be identified.

From the measurement of the energies of the fundamentals and their various combinations and of the relative intensity distribution amongst them, it is seen that the potential energy surface of the $^1B_{1u}$ electronic state is surprisingly harmonic. This fact may also account for the small numbers of examples of Fermi resonance in the anthracene spectra.

Other Lines

The lines which could not be assigned in terms of the observed a_g and b_{3g} fundamentals may be separated into the following types:

1. lines which appeared in only one of the four matrices, (a) in n-heptane, and (b) in fluorene

2. lines which appeared in more than one matrix.

Type 1 (a): in n-heptane. Some weak lines were grouped around the origin and other strong a_g modes of the $^1B_{1u}$ electronic state, as summarized in Table 10. This structure might be found in the higher quantum region, but its identification is impossible because of the appearance of much stronger combinations of the fundamentals. These weak lines have two possible interpretations. Firstly these may be a number of special sites in the lattice, each site having a different environment and giving rise to a different "solvent shift". Thus for each different environment a separate shifted spectrum should be observed; the intensity of each "shifted" spectrum would depend on the number of anthracene molecules occupying that type of site. The different possible sites that might be considered are substitutional sites, interstitial sites, sites next to a vacancy, or next to other anthracene molecules (either one or more) (47).

Table 10

Similarity of the Structure Around Some Strong Absorption Lines

	$-\Delta$ cm^{-1}									a ν_0 cm^{-1}	$+\Delta$ cm^{-1}							
	154	144		127	112	1192	80	73	43	0-0	25	47	70	85	133	146		178
										MS								
d	153		135	127	110	90	-	73	49	389	21	47	75	95	132	142	164	177
e	236		254	262	279	299		316	340	VVS	410	436	464	484	521	531	553	566
d	154		133[f]	-	116	-	-	69	51	590	26	-	73	97	-	-	-	-
e	436		457		474			521	539	S	616		663	687				
d	151		-	-	116[f]	92	76	70	-	779	19	44	78	92	139[f]	147[f]	162	176
e	628				663	687	703	709		MS	798	823	857	871	918	926	941	955
	153	144	134	127	114	91	78	71	48	$\bar{\Delta}$ cm^{-1} b.	23	46	74	92	135	145	163	177
	W	W	VW	VVW	W	VVW	VVW	W	VW	C.	S	MW	W	W	VW	VW	VW	W

a. the centers of the structure: the origin and ag fundamentals

b. average energy difference from ν_0

c. s: strong, MW: medium weak, W: weak, VW: very weak, VVW: very very weak, MS: medium strong, VVS: very very strong

d. this row shows the difference of energy value from ν_0 in cm^{-1}

e. this row shows the difference of energy value from the origin in cm^{-1}

Another possibility which must be considered is the formation of clathrate compounds. It has already been suggested by Ciais (48) and Shpol'skii (49) that saturated normal paraffin molecules form a cage about the solute molecule. Evidence favouring this point of view is found in the following experiment (50). 3.4 - benzpyrene in cyclohexane gave a diffuse spectrum at 77°K. Addition of 10% n-octane was sufficient to produce the sharp spectrum at 77°K typical of the Shpol'skii effect. If the assumption is true that clathrate compounds are formed, then the molecule may undergo free or hindered rotation. This allows an alternate explanation for the closely spaced weak lines to the blue of the origin. However there are closely spaced lines of about the same intensity to the red of the origin, and to explain the presence of these lines it is necessary to assume that the molecules rotate in the ground state. This is not possible at the low temperature used and so this explanation is not preferred.

The stronger lines about 200 cm^{-1} to the blue of the origin are hard to account for. However, if the symmetry of the crystal field at the site occupied by the anthracene molecule is lower than the molecular point group then intramolecular vibrations other than a_g or b_{3g} modes may appear. The intensities of these extra lines would depend on the strength of the coupling between the molecule with its environment. This coupling is weak in such a molecular

crystal and so perturbation theory may be applied. The interactions between solvent and solute molecules are of two kinds. There is a mixing of electronic wave functions of solvent and solute molecules giving rise to a solvent shift (20); we are not concerned with this effect here. There is also an interaction between the vibrational states of the anthracene molecule with the vibrational states of the environment which occurs in the following way. The anthracene molecule is slightly bigger in the excited state; this behaviour has already been observed in benzene (51) and naphthalene (46). The evidence in support of this conclusion is that the origin is not the strongest line in the spectrum, rather the line at 1399 cm^{-1} is. That is, the Franck-Condon overlap factor is greatest to the excited electronic state with one quantum of the 1399 cm^{-1} fundamental and so there is an expansion in the corresponding normal coordinate. However, the expansion of the anthracene molecule is felt by the surrounding molecules. Lattice motions rather than intramolecular vibrations of the solute molecule tend to be excited, because the restoring forces are much weaker between the molecules of the lattice than between the strongly bonded atoms of the molecule. Thus there is an interaction between the internal vibrations of anthracene and lattice vibrations. Application of first order perturbation theory leads directly to the result that the mixing of the states is greatest when the energy separa-

tion between them is smallest. But the frequencies of lattice modes are usually less than 100 cm^{-1}. Hence the low energy vibrational states of anthracene will be most effected. In this way low energy anthracene fundamentals of symmetry other than a_g or b_{3g} may appear. Naphthalene has low energy fundamentals of symmetry b_{1g}, b_{2g} and b_{3u} (52). The line at 420 cm^{-1} is interpreted as the overtone of the 211 cm^{-1} fundamental gaining intensity from the strong a_g fundamental at 389 cm^{-1} by Fermi resonance.

Type 1 (b) in fluorene. Most of the lines in this spectrum can be readily interpreted in terms of the anthracene fundamentals and their combinations. In fluorene the lines are broader than in n-heptane even at 4.2°K. This is especially true in higher energy regions where closely spaced combinations have not been resolved. No evidence for the presence of impurities (like carbazole which is known to form a solid solution in fluorene (40)) has been found.

The absorption spectrum of fluorene itself was observed above 31000 cm^{-1}. While the detail of this spectrum is not understood, it is apparent that the first group of lines is polarized along $\underline{c}$ axis. Thus, the low energy transition in fluorene is polarized along the long axis of the molecule.

Type 2. The low frequency intervals (about 25 cm^{-1}), built on all strong lines, are common to the spectra in all matrices. These are due to lattice modes which couple to the internal modes of anthracene as explained earlier. It

is not unexpected to find the lattice modes of different molecular crystals being about the same energy, since the frequency (ν) of a vibration is related to the force constant (k) and the reduced mass of the system (μ) by

$$\nu = \frac{1}{2\pi} (k/\mu)^{1/2}$$

The force constant (k) is directly related to bonding between the molecules which in turn is given by the heat of sublimation. The heats of sublimation for molecular crystals are of the same order of magnitude, e.g. for fluorene (53) it is 19.8 kcal/mole; biphenyl (54), 17.9 kcal/mole; naphthalene (53), 17.3 kcal/mole; n-octadecane (55), 36.8 kcal/mole. No data is available for the heat of sublimation of n-heptane but we will assume that it is about the same as for n-octadecane. The heat of sublimation is temperature dependent and the values given above were measured around room temperature. If it is assumed that the heats of sublimation at 4.2°K for all the matrices are nearly equal (and larger than the room temperature value), then we can conclude that the force constants are also within the same order of magnitude. Because the molecules considered have about the same molecular weight (fluorene, 166; biphenyl, 154; naphthalene, 128; anthracene, 178; n-heptane, 100), the reduced masses of the systems are nearly enough the same. Therefore the frequencies of the lattice modes should be very similar (fluorene, 29 cm^{-1}; n-heptane, 25 cm^{-1}; naphthalene (30), 26 cm^{-1}). Thus these low frequency

intervals are assigned as lattice modes.

In one sample of anthracene in fluorene a weak line at 73 cm^{-1} to the red of the origin was observed. This is taken to represent the presence of a ground state phonon. The intensity of this line was about one tenth that of the origin and so the temperature of this sample was about 50°K. The line was measured in an earlier spectrum in which the crystal was cemented to the helium can with silicone grease. This is further evidence that silicone grease provides poor thermal contact at low temperature.

Shift of the Origins of $^1B_{1u} \leftarrow {}^1A_g$

The energy of the $^1B_{1u} \leftarrow {}^1A_g$ transition showed a red shift as the matrix was changed from n-hexane, n-heptane, biphenyl to fluorene. And a shift was also observed in n-heptane as the temperature was lowered as seen in Table 5. According to McClure (20) dispersion forces between host and guest molecules causes the energy shift, and his calculations for the $^1B_{1u} \leftarrow {}^1A_g$ transition of anthracene in the vapour phase and in solid matrices of naphthalene and phenanthrene show fairly good agreement with experiment (30). Since the fluorene molecule is slightly polar, this interpretation gives reasonable agreement with our result.

BIBLIOGRAPHY

1 D.P. Craig and P.C. Hobbins, J. Chem. Soc. 1955, 539.

2 S.I. Weissman, J. Chem. Phys. 18, 232 (1950)

3 T. Forster, Z. Phys. Chem. 41, 287 (1938)

4 C.A. Coulson, Proc. Phys. Soc. (London) A60, 257 (1948)

5 W. Moffitt, J. Chem. Phys. 22, 320 (1954)

6 M.J.S. Dewar and H.C. Longnet-Higgins, Proc. Phys. Soc. (London) A67, 795 (1954)

7 J.A. Pople, Proc. Phys. Soc. (London) A68, 81 (1955)

8 R. Pariser, J. Chem. Phys. 24, 250 (1956)

9 N.S. Ham and K. Rudenberg, J. Chem. Phys. 25, 1 (1956)

10 N. Mataga, Bull. Chem. Soc. Japan 31, 463 (1958)

11 H. Foetz and E. Heilbrowner, Helv. Chim. Acta 44, 1365 (1961)

12 R.L. Hummel and K. Ruedenberg, J. Phys. Chem. 66, 2334 (1962)

13 J. Koutecky, J. Paldus, and R. Zahradnik, J. Chem. Phys. 36, 3129 (1962)

14 E. Fermi, Z. Physik, 71, 250 (1931)

15 D.P. Craig, J. Chem. Soc. 1955, 2302

16 D.P. Craig, J. Chem. Soc. 1950, 2146 (1950)

17 J.B. Coon, R.E. DeWames and C.M. Loyd, J. Mal. Spect. 8, 285 (1962)

18 D.P. Craig and T. Thirunamachandran, Pro. Roy. Soc. A271, 207 (1963)

19 D.P. Craig and T. Thirumamachandran, Pro. Chem. Soc. 1961, 253 (1961)

20 D.S. McClure, Symposium on on electrical conductivity in organic solids (April, 1960)

21 D.P. Craig and H.S. Walmsley, Mal. Phys. 4, 113 (1961)

22 E.V. Shpolskii, Usp. Fiz. Nauk 71, 215 (1960)

23 E.V. Shpolskii, Usp. Fiz. Nauk 77, 321 (1962)

24 K.K. Rebane and V.V. Khizhnyakov, Optics and Spectroscopy 14, 193 (1962)

25 Ibid., 14, 262 (1963)

26 G. Kortum and B. Finckin, Z. physik. Chem. B52, 263 (1942)

27 E. Clar, Spectrochim Acta 4, 116 (1950)

28 T.N. Bolotnikova, Izvest. Akad. Nauk SSSR, Ser. Fiz. 23, 29 (1959)

29 J.W. Sidman, Phys. Rev. 102, 96 (1956)

30 J.W. Sidman, J. Chem. Phys. 25, 115 (1956)

31 L. Columbo et J.P. Mathieu, Bull. Soc. Franz. Miner. Crist. LXXXIII, 250 (1960)

32 W. Bruhn and R. Mecke, Z. Elektrochemie 65, 543 (1961)

33 S. Califano, J. Chem. Phys. 36, 903 (1962)

34 S.K. Lower Ph.D. thesis

35 G.K. White, Experimental Techniques in Low-Temperature Physics (Oxford, 1959)

36 J. Ferguson, private communication

37 W.R. Brode, Chemical Spectroscopy (John Willey and Sons, 1946)

38 H. Kayser, Tabelle der Schwingungszahlen (S. Hirzel, 1925)

39 E.R. Lippincott and E.J. O'Reily Jr., J. Chem. Phys. 23, 238 (1955)

40 M. Brandstatter - Kuhnert and H. Weiss, Monatsh. 88, 1007 (1957)

41 H. Zimmermann and N. Joop, Z. Elektrochemie 65, 66 (1961)

42 R.M. Hochstrasser and R. Zwarich, private communication

43 R.N. Nurmukhametov and G.V. Gobov, Optika i Spektroskopiya 13, 676 (1962)

44 E.J. Bowen, N.J. Holder, and G.B. Woodger, J. Phys. Chem. 66, 2491 (1962)

45 N.A. Borisenich and V.V. Gmzinskii, Izvest. Akad. Nauk SSSR Ser. Fiz. 24, 545 (1960)

46 D.P. Craig and J.M. Hollas, et al., Phylosophical translations of the Royal Society of London, A253, 543 (1961)

47 R.E. Behringer, J. Chem. Phys. 29, 537 (1958)

48 A. Ciais, J. Chem. Phys. 58, 190 (1961)

49 E.V. Shpol'skii, Soviet Physics Uspekhi 6, 411 (1963)

50 B. Muel and G. Lacroix, Bull. Soc. Chim. France, 2139 (1960)

51 D.P. Craig, J. Chem. Soc. 1950, 2146

52 J.M. Hollas, J. Molecular Spect. 9, 138 (1962)

53 Bradley and Cleasby, J. Chem. Soc. 1953, 1690

54 A. Aihara, J. Chem. Soc. Japan, Pure Chem. Sect. 76, 492 (1955)

55 Bradley and Shellard, Proc. Roy. Soc. A198, 239 (1949)